OPEN

Inactivation of the E3 Ubiquitin Ligase IDOL Attenuates Diet-Induced Obesity and Metabolic Dysfunction in Mice

Nienke M. van Loon, Roelof Ottenhoff, Sander Kooijman, Martina Moeton, Saskia Scheij, Reinout L.P. Roscam Abbing, Marion J.J. Gijbels, Johannes H.M. Levels, Vincenzo Sorrentino, Jimmy F.P. Berbée, Patrick C.N. Rensen, Noam Zelcer

Objective—The E3 ubiquitin ligase IDOL (inducible degrader of the LDLR [LDL (low-density lipoprotein) receptor]) is a post-transcriptional regulator of LDLR abundance. Model systems and human genetics support a role for IDOL in regulating circulating LDL levels. Whether IDOL plays a broader metabolic role and affects development of metabolic syndrome-associated comorbidities is unknown.

Approach and Results—We studied WT (wild type) and *Idol*$^{(-/-)}$ (Idol-KO) mice in 2 models: physiological aging and diet-induced obesity. In both models, deletion of *Idol* protected mice from metabolic dysfunction. On a Western-type diet, *Idol* loss resulted in decreased circulating levels of cholesterol, triglycerides, glucose, and insulin. This was accompanied by protection from weight gain in short- and long-term dietary challenges, which could be attributed to reduced hepatosteatosis and fat mass in Idol-KO mice. Although feeding and intestinal fat uptake were unchanged in Idol-KO mice, their brown adipose tissue was protected from lipid accumulation and had elevated expression of UCP1 (uncoupling protein 1) and TH (tyrosine hydroxylase). Indirect calorimetry indicated a marked increase in locomotion and suggested a trend toward increased cumulative energy expenditure and fat oxidation. An increase in in vivo clearance of reconstituted lipoprotein particles in Idol-KO mice may sustain this energetic demand. In the BXD mouse genetic reference population, hepatic *Idol* expression correlates with multiple metabolic parameters, thus providing support for findings in the Idol-KO mice.

Conclusions—Our study uncovers an unrecognized role for Idol in regulation of whole body metabolism in physiological aging and on a Western-type diet. These findings support Idol inhibition as a therapeutic strategy to target multiple metabolic syndrome-associated comorbidities.

Visual Overview—An online visual overview is available for this article. **(*Arterioscler Thromb Vasc Biol*. 2018;38:1785-1795. DOI: 10.1161/ATVBAHA.118.311168.)**

Key Words: adipose tissue, brown ■ cholesterol ■ lipid metabolism ■ metabolic syndrome ■ obesity ■ ubiquitin-protein ligases

The metabolic syndrome—a condition associated with a variety of comorbidities, including dyslipidemia, fatty liver disease, obesity, and diabetes mellitus—is a major population-wide health problem. This is highlighted by reports from the World Health Organization and the International Diabetes Federation indicating that 39% of the world population is overweight, >425 million worldwide are experiencing diabetes mellitus, and ≈25 million yearly deaths are attributed to cardiovascular diseases. Treating these diseases is putting a heavy burden on already limited healthcare resources, thereby emphasizing the need to improve our understanding of the underlying pathophysiologic mechanisms and to identify novel therapeutic targets and strategies. Ideally, such targets would be able to address multiple morbidities associated with the metabolic syndrome.

The LDLR (LDL [low-density lipoprotein] receptor) is a key determinant of the level of circulating plasma lipoproteins.[1] However, recent studies suggest that the LDLR may also play a role in the pathophysiology of obesity and diabetes mellitus. Patients with familial hypercholesterolemia because of loss-of-function mutations in the *LDLR* or *APOB* (apoliporprotein B) genes show a reduced incidence of type 2

Received on: April 10, 2018; final version accepted on: May 31, 2018.

From the Department of Medical Biochemistry (N.M.v.L., R.O., M.M., S.S., M.J.J.G., N.Z.), Tytgat Institute for Liver and Intestinal Research (R.L.P.R.A.), and Department of Experimental Vascular Medicine (J.H.M.L.), Academic Medical Center, University of Amsterdam, The Netherlands; Division of Endocrinology, Department of Medicine, Einthoven Laboratory for Experimental Vascular and Regenerative Medicine, Leiden University Medical Center, The Netherlands (S.K., J.F.P.B., P.C.N.R.); Department of Pathology (M.J.J.G.) and Department of Molecular Genetics (M.J.J.G.), CARIM, Maastricht University, The Netherlands; and Laboratory for Integrative and Systems Physiology, EPFL, Lausanne, Switzerland (V.S.).

The online-only Data Supplement is available with this article at https://www.ahajournals.org/journal/atvb/doi/suppl/10.1161/atvbaha.118.311168.

Correspondence to Noam Zelcer, PhD, Department of Medical Biochemistry, Academic Medical Center of the University of Amsterdam, Meibergdreef 9, 1105AZ Amsterdam, The Netherlands. E-mail n.zelcer@amc.uva.nl

Nonstandard Abbreviations and Acronyms	
BAT	brown adipose tissue
DM2	type 2 diabetes mellitus
HDL	high-density lipoprotein
HET	heterozygous
IDOL	inducible degrader of the low-density lipoprotein receptor
KO	knockout
LDL	low-density lipoprotein
LDLR	low-density lipoprotein receptor
PCSK9	proprotein convertase subtilisin/kexin type 9
TG	triglyceride
TH	tyrosine hydroxylase
UCP1	uncoupling protein 1
WAT	white adipose tissue
WT	wild type
WTD	Western-type diet

diabetes mellitus (DM2).[2] In contrast, the use of cholesterol-lowering statins, which increase abundance of the LDLR, is associated with an elevated incidence of DM2.[3–5] Targeting PCSK9 (proprotein convertase subtilisin/kexin type 9)[6]—a novel cholesterol-lowering strategy that is also based on increasing the level of the LDLR—has not been associated with increased DM2 yet. However, single-nucleotide polymorphisms in *PCSK9* that are associated with lower circulating LDL cholesterol have been associated with an increased incidence of DM2, bodyweight, and waist-to-hip ratio.[7,8] These findings are in line with studies in mice, where genetic ablation of *Pcsk9* led to increased plasma levels of glucose with concomitant reduced insulin levels.[9,10] Taken together, these studies support the notion that beyond its role in hypercholesterolemia, the LDLR could play a role in the pathogenesis of the metabolic syndrome as well.

We have recently identified the IDOL (inducible degrader of the LDLR, also known as MYLIP [myosin light chain interacting protein]) as a post-transcriptional regulator of LDLR abundance.[11–13] Unlike PCSK9 that recognizes the ectodomain of the LDLR and the related receptors VLDLR (very low-density lipoprotein receptor) and APOER2 (apolipoprotein E receptor 2),[14] IDOL recognizes the intracellular tail of these receptors, and acting as an E3 ubiquitin ligase promotes their ubiquitylation and subsequent lysosomal degradation.[15] In mice, Idol has a limited impact on plasma LDL—an outcome that is likely because of limited sterol-dependent regulation of *Idol* in mouse liver.[16] In contrast, in nonhuman primates, gain or loss of IDOL function increases and decreases LDL levels,[16] respectively, and we have recently reported that human carriers of a loss-of-function mutation in *IDOL* have lower circulating LDL levels.[17] However, although regulation of the LDLR by IDOL is established, it is unknown whether IDOL affects systemic lipid and energy metabolism. To address this issue, we investigated the metabolic phenotype of *Idol*$^{(-/-)}$ (Idol-KO) mice in response to a Western-type diet (WTD), which contains fat and cholesterol, and during physiological aging. We report that Idol-KO mice are protected from diet-induced obesity and associated detrimental metabolic changes, highlighting the potential of targeting IDOL in metabolic disease.

Materials and Methods

The data that support the findings of this study are available from the corresponding author on reasonable request

Animal Studies

Handling of mice was done according to institutional guidelines and regulations, and all efforts were made to minimize suffering. Approval for these experiments was obtained before conducting the experiments from the Institutional Ethical Committee on Animal Experimentation of the Academic Medical Center. The generation of the Idol-KO mice was reported previously, and the mice were kindly provided by Peter Tontonoz (University of California at Los Angeles)[16] (please see the major resources table in the online-only Data Supplement). To follow physiological aging (experiment I), male and female Idol WT (wild type), HET (heterozygous), and KO (knockout) mice were weaned at 3 weeks of age (n=5–6 mice per group), group housed, and fed a chow diet ad libitum (Teklad 2916; Envigo, The Netherlands). Mice were weighed biweekly by animal facility staff that were blinded to genotype or outcome. Blood glucose levels were measured at the age of 7 months after 4 hours of fasting. At the age of 12 months, mice were euthanized, blood was drawn by heart puncture, and organs were collected and snap-frozen in liquid nitrogen and stored at −80°C or fixed in phosphate buffered 4% paraformaldehyde. To evaluate the response to a WTD (experiments II and III), mice were fed a diet containing 60% fat and 0.2% cholesterol (open source diet D12492 with 0.2% cholesterol; 60 kcal% fat, 20 kcal% carbohydrates, and 20 kcal% protein; Ssniff Diets, Germany). Six- to 8-week-old male Idol-KO (n=9) and WT (n=12) mice were group housed with siblings of the same genotype and fed WTD for 5 months (experiment II). The mice were weighed weekly. At the indicated time points, mice were fasted for 4 hours, and blood glucose was measured with a glucometer (Bayer Contour XT). Oral glucose tolerance tests were performed at 8 and 20 weeks of WTD by fasting mice for 4 hours followed by oral loading with 2.0 g glucose per kg body weight. Tail vein blood was sampled at the indicated time points and glucose measured with a glucometer. At euthanization, plasma and organs were collected and stored as described above. Organs were collected snap-frozen in liquid nitrogen and stored at −80°C or fixed in phosphate buffered 4% paraformaldehyde, paraffin embedded, and sectioned. In an independent experiment (experiment III), conducted in the animal facility of Leiden University Medical Center, male Idol-KO (n=11) and WT mice (n=8) rederived to specific organism and pathogen-free status were used. Starting from 8 weeks of age, all mice were fed a WTD as above. After 4 weeks of WTD, mice were placed individually in a metabolic cage (Phenomaster line; TSE Systems, Bad Homburg, Germany) for 4 days. Subsequently, after 4 hours of fasting, mice were intravenously injected with 80-nm-sized lipoprotein-like emulsion particles containing glycerol tri[^{3}H]oleate and [^{14}C]cholesteryl oleate, as described previously,[18] and blood samples were drawn from the tail vein at the indicated times. Clearance of the injected radiolabeled tracers was calculated as the percentage of the total injected dose. Directly hereafter, mice were euthanized by cervical dislocation, perfused with ice-cold PBS, and organs were isolated and weighed. Uptake of the radiolabels was determined by scintillation counting after organs were dissolved. To assess the postprandial response, we measured the appearance of plasma triglycerides (TG) following an oral olive oil gavage. Briefly, male Idol WT and KO (n=6 per group) mice of 10 to 12 weeks were fasted for 4 hours (9 AM), after which they received an oral load of 400 µL olive oil (1 PM). Subsequently, blood samples were drawn from the tail vein into EDTA-coated tubes (CB300, Sarstedt) at the indicated time points after gavage. To assess hepatic VLDL (very low-density lipoprotein) secretion, male mice (n=3 per group) were fasted for 4 hours (8 AM), after which they received an intraperitoneal injection of Poloxamer 470 (1 g/kg) and blood samples collected as above. For both the olive oil gavage and poloxamer experiments, samples were kept on ice, spun down at 4000 rpm for 7 minutes at 4°C, and plasma was assessed for TG. In all experiments, mice were housed in a light- and temperature-controlled room in the animal facilities of the Academic Medical Center or Leiden University Medical Center.

Analysis of BXD Mouse Strain Panel

Male mice of both parental strains (C57BL/6 and DBA/2) and 40 of their intermediate BXD strains (BXD43-BXD103) were bred and born at the EPFL, Switzerland (n=5 per strain).[19] These recombinant inbred mouse strains, derived from an intercross of the 2 parental mouse strains above, have been extensively used to interrogate genotype-phenotype associations. From the age of 8 weeks onward, animals were fed a high-fat diet (60% kcal fat) for a total of 5 months. Metabolic phenotyping was performed between the age of 16 and 24 weeks. After 5 months of high-fat diet, animals were fasted overnight and euthanized by means of perfusion following isoflurane anesthesia. Livers were snap-frozen in liquid nitrogen. RNA was pooled per strain before purification and array analysis. Spearman rho correlation analyses where performed using the data available on GeneNetwork (www.genenetwork.org) and R as described previously.[20]

Analysis of Plasma

Insulin (10-1247-01, Mouse Insulin ELISA; Mercodia, Sweden), glucose (101192, Glucose-TR, Spinreact), aspartate aminotransferase (AST; 92025, AST TGO Colorimetric Method; Biolabo, France), and alanine transaminase (ALT; 92027; TGP Colorimetric Method; Biolabo, France) levels were determined in plasma samples following manufacturers' protocols. Concentrations of circulating lipids were measured using commercially available enzymatic kits for TG (11488872; Roche Diagnostics, Mannheim, Germany), total cholesterol (TC; 11489232, Roche Diagnostics), and phospholipids (3009, Instruchemie; Delfzijl, The Netherlands). HDL (high-density lipoprotein) cholesterol was measured after precipitation of ApoB-containing lipoproteins by polyethylene glycol 6000.

Fast Protein Liquid Chromatography Analysis of Plasma Lipoproteins

TC and TG content from the main plasma lipoprotein classes (VLDL, LDL, and HDL) was determined using fast protein liquid chromatography as described previously.[21] Briefly, the system contained a PU-980 ternary pump with an LG-980-02 linear degasser, FP-920 fluorescence, and UV-975 UV/VIS detectors (Jasco, Tokyo, Japan). An extra PU-2080i Plus pump (Jasco, Tokyo, Japan) was used for either in-line cholesterol PAP or TG enzymatic reagent (Roche, Basel, Switzerland) addition at a flow rate of 0.1 mL/min. Plasma lipoproteins were separated using a Superose 6 HR 10/30 column (GE Healthcare, Hoevelaken, The Netherlands) using Tris-buffered saline pH 7.4, as eluent at a flow rate of 0.31 mL/min. Commercially available lipid plasma standards (low, medium, and high) were used for generation of TC or TG calibration curves for the quantitative analysis (SKZL, Nijmegen, The Netherlands) of the separated lipoprotein fractions. Quantitative analysis of the chromatograms was performed with ChromNav chromatographic software, version 1.0 (Jasco, Tokyo, Japan).

Quantitative Polymerase Chain Reaction Analysis

RNA was isolated from powdered tissue samples in TriReagent (Sigma) with an RNA extraction kit (R2052, Zymo Research), which included a DNAse treatment, and subsequently transcribed to cDNA with the biotool cDNA synthesis kit (B24403, Biotool). Quantitative polymerase chain reaction was performed using Sensifast SYBR Green (Bioline BIO-98020) on a Lightcycler 480 system (Roche). Gene expression was normalized to the mean expression of Rplp0 and Rpl13. Primer sequences are available on request.

Immunohistochemistry Procedures

Fixed tissues were embedded, sectioned, and stained for hematoxylin and eosin, and frozen tissues were sectioned and stained with Oil Red O at the Department of Pathology of the Academic Medical Center. Slides were assessed and scored by a blinded mouse pathologist (M.J.J.G.). Adipocyte diameter was determined using the Adiposoft plugin for FIJI.[22] Staining of UCP1 (uncoupling protein 1) and TH (tyrosine hydroxylase) was done as described previously.[23,24] No background staining was observed for both antigens when the primary antibody was replaced by purified immunoglobulins (not shown). Briefly, sections were dewaxed, rehydrated, and treated with peroxidase. Antigen retrieval was accomplished in 10 mmol/L citrate buffer (pH=6.0). Slides were blocked with normal goat serum (UCP1) or BSA (TH) and incubated overnight at 4°C with anti-UCP1 antibodies (1:4000; Ab10983; Abcam, Cambridge, United Kingdom) or anti-TH antibodies (1:2000; Ab112; Abcam). Next, sections were incubated for 30 minutes with biotinylated goat α-rabbit secondary antibodies (UCP1; 1:600; Vector Laboratories, Burlingame, CA) or DAKO EnVision anti-rabbit antibodies (DAKO, Glostrup, Denmark). Immunostaining was amplified and visualized using the Elite ABC Nova Red kit (Vector Laboratories). Counterstaining was performed with Mayer hematoxylin (1:4). Staining was quantified blindly in FIJI after color deconvolution to extract DAB (3,3'-diaminobenzidine) staining.

Statistical Analysis

Data are presented as mean±SEM. After testing for normality and equal variance, unpaired *t* tests or unpaired repeated *t* tests with Holm-Sidak correction were conducted or alternatively a nonparametric Mann-Whitney analysis was performed (GraphPad Prism 6.0). A $P < 0.05$ was considered statistically significant. Correlations were assessed using Spearman correlations.

Results

Idol-KO mice are viable, and their initial description reported no overt phenotype.[16] Given the important metabolic role of the known Idol degradation targets,[15] we decided to evaluate the short- and long-term response of male Idol-KO mice to a WTD containing fat and cholesterol. Diet-induced weight gain was significantly lower in Idol-KO compared with WT mice in both the short-term and long-term experiments (5 weeks, Figure 1A, and 21 weeks, Figure 1B; Figure IA in the online-only Data Supplement). In these experiments, no differences in food intake were observed between the genotypes (Figure 4A and not shown). The difference in diet-induced weight gain between Idol-KO and WT mice could be primarily attributed to reduced liver and fat mass (Figure 1C). Concomitantly, plasma levels of glucose and insulin were also reduced in Idol-KO mice as compared with WT mice, reaching significance when mice were followed for 21 weeks (Figure 1D through 1F). The primary target of Idol—the LDLR—is a key regulator of circulating lipoprotein levels.[1] Accordingly, in the absence of Idol, we found that there was a reduction in the level of circulating TG and phospholipids (Figure 1G and 1H), as well as of TC (Figure 1I). Analysis of plasma lipoproteins indicated that the reduction in cholesterol in Idol-KO mice was associated with a prominent decrease in both the HDL and LDL fractions as compared with WT mice (Figure 1J and 1K). At the later WTD time point, the decrease in plasma TG was blunted, yet TC levels remained significantly lower in Idol-KO mice (Figure 1L; Figure IB and IC in the online-only Data Supplement).

These findings with the WTD prompted us to also evaluate the phenotype of chow-fed Idol-KO mice of both genders. Initially, the body weights of male and female chow-fed Idol-KO mice were indistinguishable from those of their WT controls (Figure IIA in the online-only Data Supplement). However, from 22 weeks of age onward, Idol-KO females maintained their body weight unlike WT female mice that continued to gain weight. Female, but not male, Idol-HET mice showed an intermediate weight phenotype suggesting

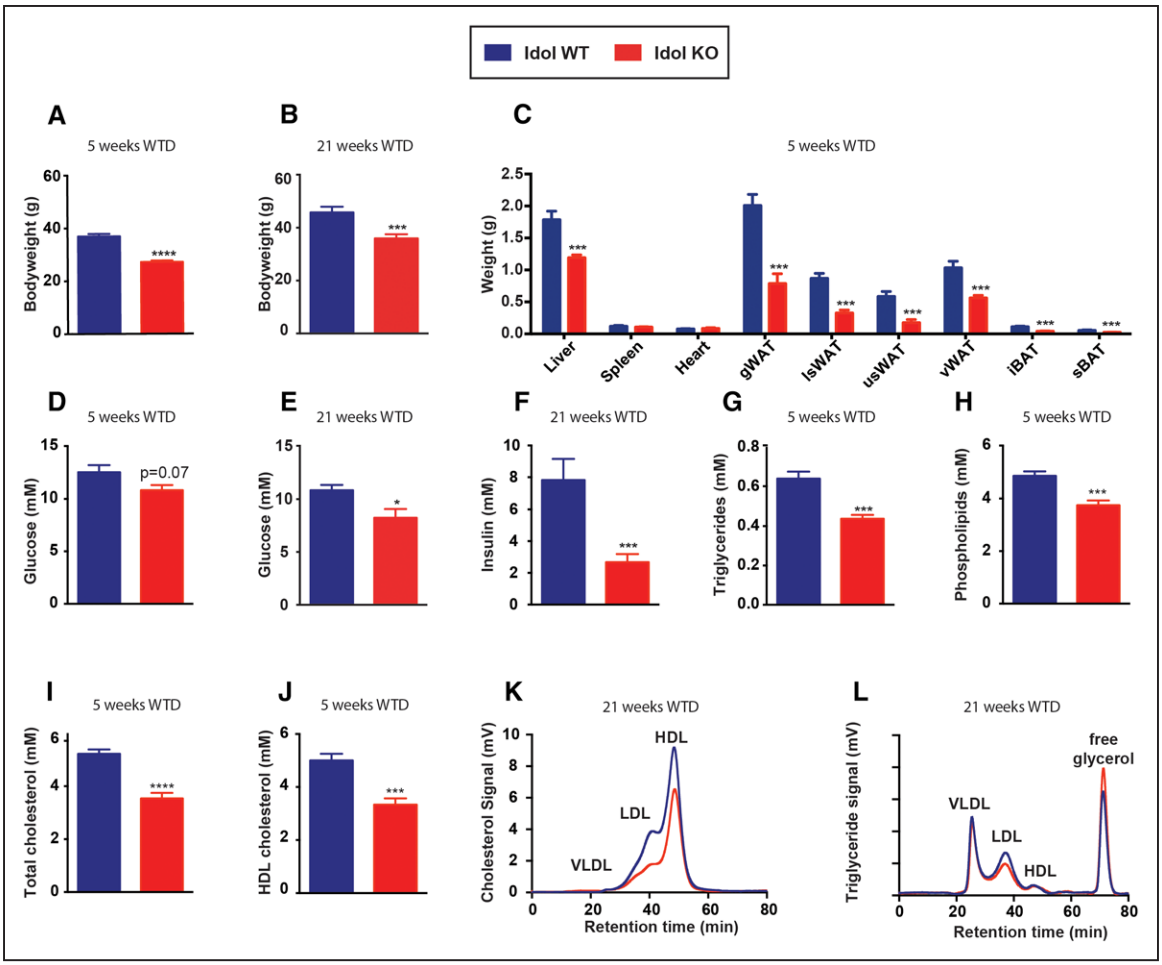

Figure 1. Idol (inducible degrader of the low-density lipoprotein receptor) deficiency improves metabolic control on a Western-type diet (WTD). WT (wild type) and IDOL-KO (knockout) male mice were fed a 60% fat 0.2% cholesterol diet for 5 or 21 wk, as indicated (n=8–11). **A** and **B**, Total bodyweight and (**C**) weight of individual tissues is shown. The level of fasted plasma (**D** and **E**) glucose, (**F**) insulin, (**G**) triglycerides (**H**), phospholipids (**I** and **J**), and of total cholesterol and HDL (high-density lipoprotein) cholesterol is plotted. **K** and **L**, Plasma was fractionated and cholesterol and triglyceride content of the different lipoprotein fractions determined. Each bar and error represent the mean±SEM. gWAT indicates gonadal white adipose tissue; iBAT, interscapular brown adipose tissue; lsWAT, lower subcutaneous white adipose tissue; sBAT, subscapular brown adipose tissue; usWAT, upper subcutaneous white adipose tissue; and vWAT, visceral white adipose tissue. **P*<0.01, ****P*<0.001, *****P*<0.0001.

a dose-dependent Idol effect in females. Moreover, chow-fed female Idol-KO mice also had a significantly reduced blood glucose level as compared with WT controls (Figure IIB in the online-only Data Supplement). Lower glucose levels were only observed in male Idol-KO mice following a WTD (Figure 1E; Figure IIB in the online-only Data Supplement). Yet, despite this observation, the response of WTD-fed male Idol-KO mice to oral glucose loading was indistinguishable from that of WT mice, both after 8 and 20 weeks of diet (Figure III in the online-only Data Supplement). In aggregate, these findings suggest that the absence of Idol attenuates several important aspects of the metabolic syndrome in mice.

Because the difference in weight gain could be largely attributed to the liver and fat depots, we examined these tissues in more detail. WTD feeding of male WT mice resulted in prominent appearance of hepatic vacuoles that stained for neutral lipids (Figure 2A), without hepatic toxicity as determined by plasma AST and ALT levels (Figure IV in the online-only Data Supplement). In contrast, livers of male Idol-KO mice were largely protected from diet-induced fat accumulation, as evident from a blinded pathological evaluation of the livers (Figure 2A and 2B). Hepatic lipid accumulation was not evaluated in chow-fed male Idol-KO mice and was lower in chow-fed female Idol-KO mice when compared with their female WT controls (data not shown). The reduced hepatic fat accumulation in WTD-fed Idol-KO male mice was associated with a lower liver weight (Figure 2C), likely because of decreased hepatic TG accumulation (Figure 2D). In contrast, hepatic cholesterol was slightly increased in livers of WTD-fed male Idol-KO mice in the absence of liver toxicity (Figure 2E; Figure IV in the online-only Data Supplement). Unexpectedly, despite the marked difference between the livers of WT and Idol-KO mice, hepatic gene expression was comparable across a wide range of genes involved in lipid metabolism, and the level of hepatic LDLR protein was not significantly different (Figure 2F and not shown). In fact, the 1 gene that we found to be differentially expressed was *Cyp7a1*, which may be an outcome of increased hepatic cholesterol levels in the livers of Idol-KO mice.[25]

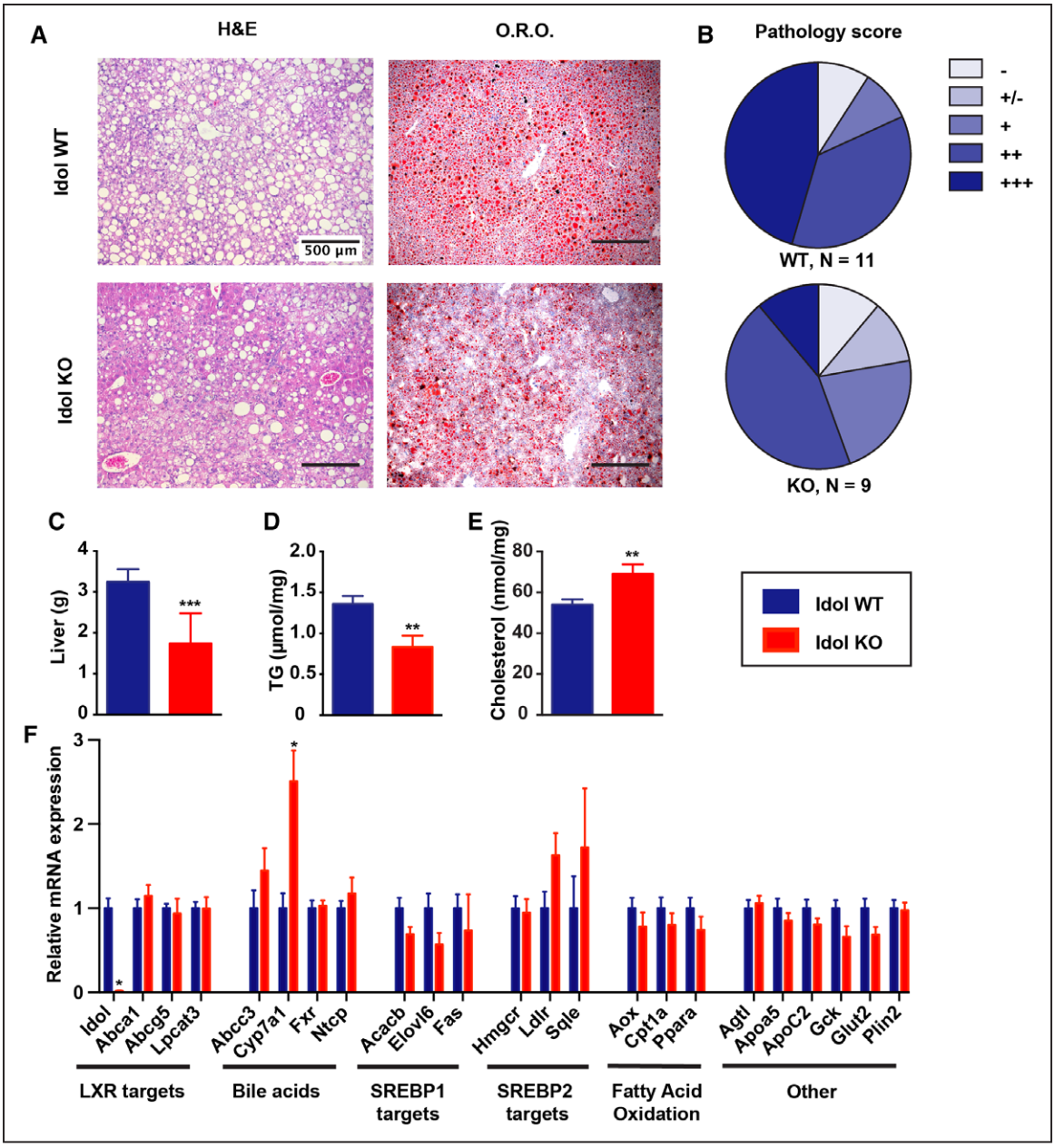

Figure 2. Loss of Idol (inducible degrader of the low-density lipoprotein receptor) limits hepatic triglyceride (TG) accumulation on a Western-type diet (WTD). WT (wild type) (n=11) and Idol-KO (knockout; n=9) male mice were fed a WTD for 21 wk. **A**, Representative (**left**) hematoxylin and eosin (H&E) and (**right**) Oil Red O (ORO) staining of liver sections from Idol WT and KO mice. **B**, Blinded macropathological scoring of vacuole size in H&E sections. Semiquantitative scale ranging from (–) no vacuoles to (+++) in which no hepatic zonation can be distinguished. Liver (**C**) weight, (**D**) TG content, and (**E**) cholesterol content in WT and Idol-KO mice. **F**, Hepatic mRNA expression of the indicated genes sorted by functional class. Expression of indicated genes was normalized, and the value in WT mice was set to 1. Each bar and error represent the mean±SEM. **P*<0.01, ***P*<0.001. LXR indicates liver X receptor; and SREBP, sterol regulatory element-binding protein.

Next to the liver, fat depots were the most affected tissues in Idol-KO mice in response to the WTD (Figure 1C). Accordingly, histological inspection of gonadal white adipose tissue (WAT) revealed a marked difference between WT and Idol-KO mice, as also reflected in the increased fat cell size in this depot (Figure 3A). A striking difference between the genotypes was also observed in brown adipose tissue (BAT), with WT BAT showing prominent accumulation of lipids that was nearly absent in Idol-KO BAT (Figure 3B). Two key determinants of thermogenic BAT activity are UCP1 levels and peripheral sympathetic neurosignaling for which the level of the enzyme TH can be used as a proxy.[26,27] Both of these markers were clearly present in Idol-KO BAT, but were close to absent in WT controls, consistent with the massive accumulation of lipid in these mice (Figure 3C and 3D; Figure V in the online-only Data Supplement).

The reduced weight gain and decreased lipid accumulation in adipose tissue and liver of Idol-KO mice prompted us to explore the potential underlying mechanism(s). We considered the possibility that in the absence of Idol, intestinal absorption of dietary fat would be decreased, explaining these observations. To test this idea, we challenged male mice with

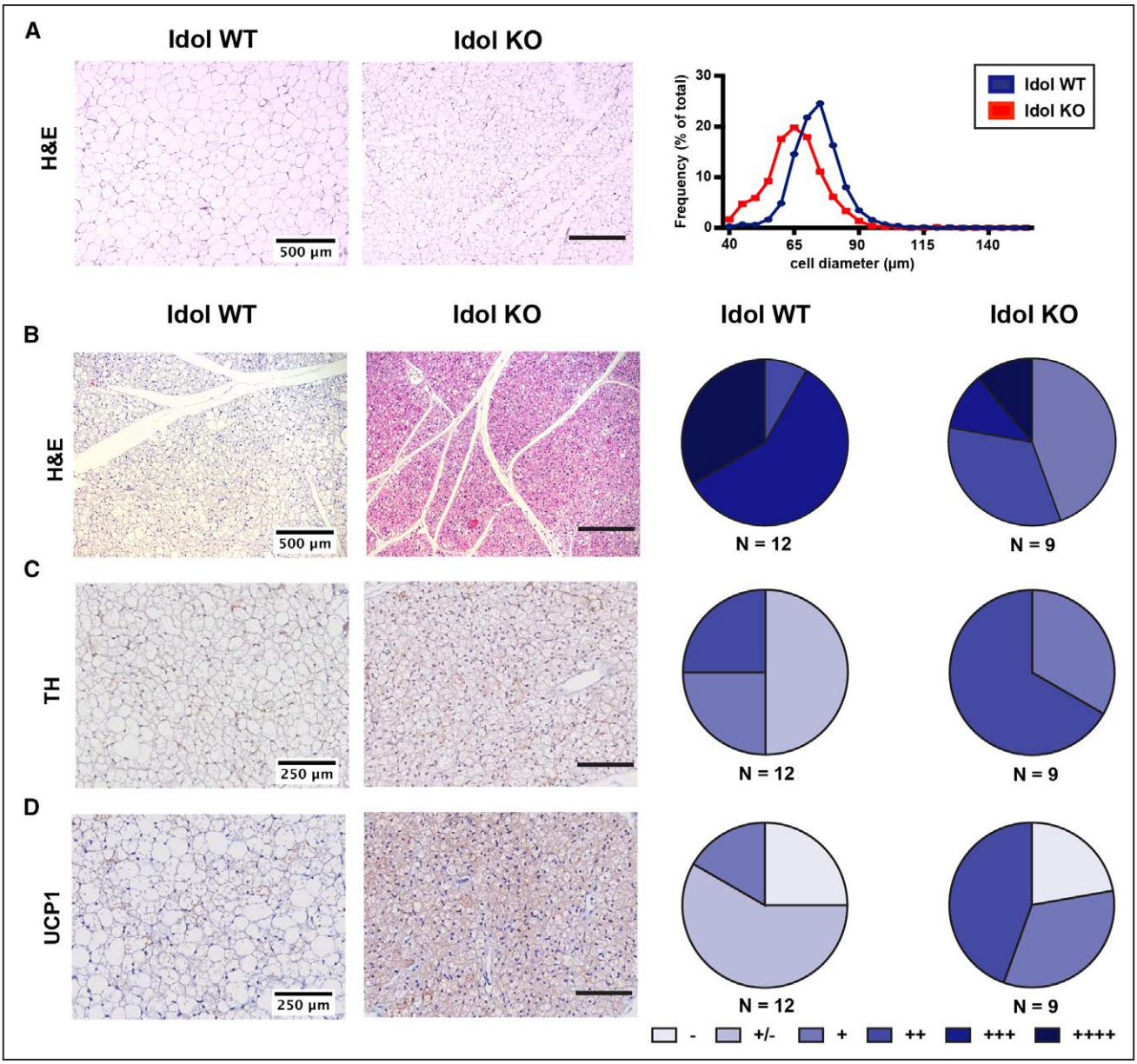

Figure 3. Absence of Idol (inducible degrader of the low-density lipoprotein receptor) attenuates Western-type diet (WTD)-induced alterations in adipose tissue depots. WT (wild type; n=11) and Idol-KO (knockout; n=9) male mice were fed a WTD for 21 wk. **A**, Representative hematoxylin and eosin (H&E) staining (**left**) and frequency distribution of adipocyte cell diameter (**right**) of gonadal white adipose tissue. Representative images of (**B**) H&E staining and immunostaining of (**C**) tyrosine hydroxylase (TH) and (**D**) UCP1 (uncoupling protein 1) in brown adipose tissue of WT and Idol-KO mice. (**B**–**D**; **right**) Blinded macropathological scoring of (**B**) lipid accumulation, and (**C** and **D**) TH and UCP1 staining, respectively, using a semiquantitative scale ranging from absent (–) to prominent (++++).

an oral olive oil bolus and measured the time-dependent levels of circulating TG. This offers a gross assessment of intestinal fat uptake, packaging into chylomicrons, and subsequent basolateral secretion, although it has to be noted that the measured levels also integrate, for example, tissue clearance. In this experimental setting, no differences in postprandial plasma TG levels were observed in Idol-KO mice (Figure VIA in the online-only Data Supplement). Similarly, we measured no difference in plasma TG after Poloxamer 470 injection in male mice, suggesting that hepatic VLDL secretion between WT and Idol-KO mice is an unlikely explanation for the reduced accumulation of TG in the liver of Idol-KO mice (Figure VIB in the online-only Data Supplement). An alternative scenario that could underlie the metabolic phenotype of Idol-KO mice is increased energy expenditure, which is in line with maintained BAT in these mice. To evaluate this notion, we fed male WT and Idol-KO mice a WTD for 5 weeks and measured their energy expenditure by means of indirect calorimetry. Importantly, in the course of this experiment, food intake was comparable between the 2 genotypes (Figure 4A), ruling out feeding behavior as a confounding parameter in these studies. In contrast, Idol-KO mice had a marked increase in locomotor activity as determined by the number of beam breaks during the course of these experiments (Figure 4B). Energy expenditure (Figure 4C and 4D) and fat oxidation (Figure 4E through 4H) seemed higher in Idol-KO compared with WT

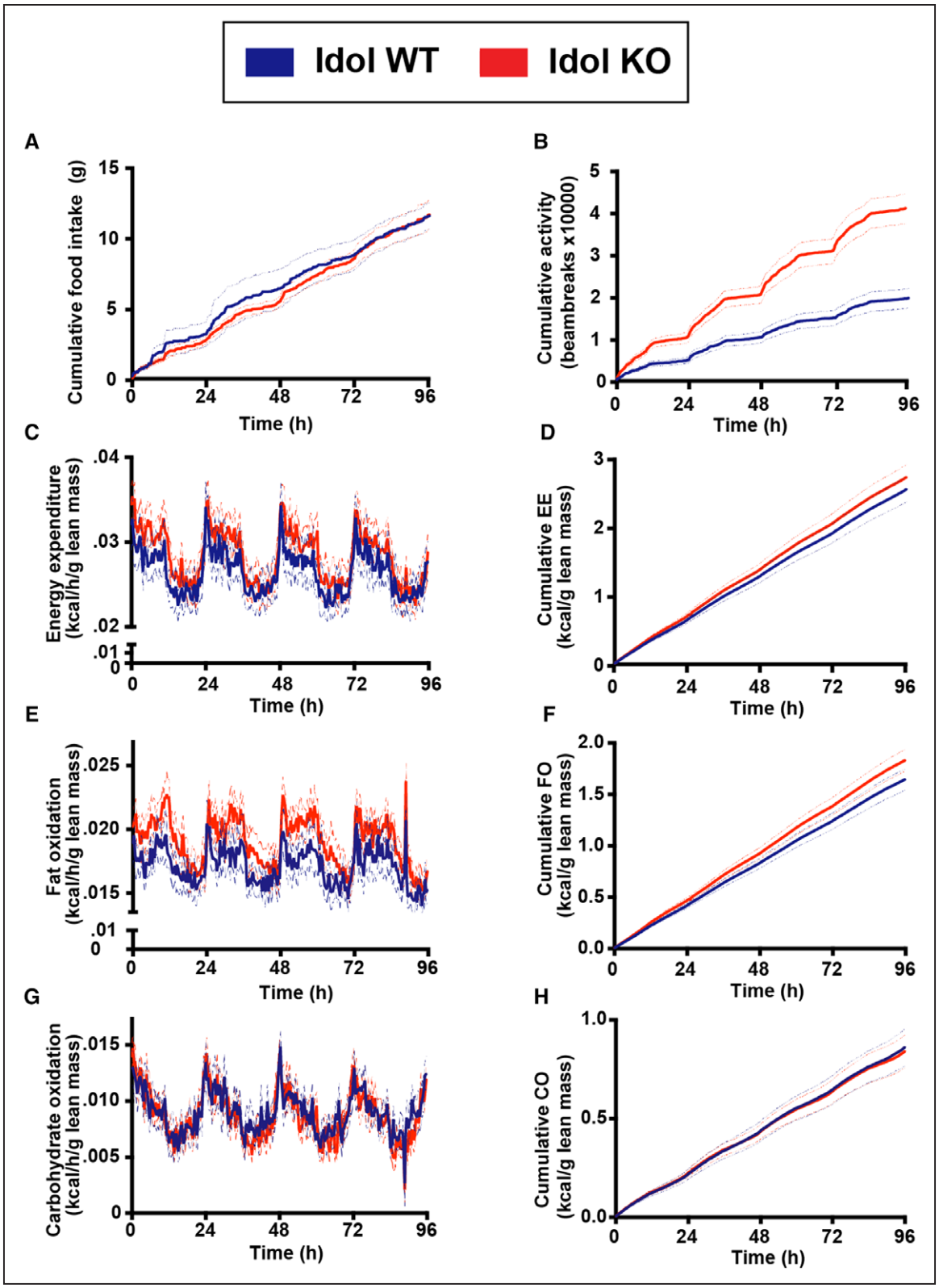

Figure 4. Indirect calorimetry in Western-type diet (WTD)-fed Idol (inducible degrader of the low-density lipoprotein receptor)-KO (knockout) mice. WT (wild type; n=8) and Idol-KO (n=11) male mice were fed a WTD for 5 wk, after which they were housed individually in metabolic cages for 4 consecutive days. The cumulative (**A**) food intake and (**B**) locomotor activity (expressed as the number of beam breaks) in WT and Idol-KO is plotted. The lean mass-corrected time-dependent and cumulative, respectively (**C** and **D**), energy expenditure (EE; **E** and **F**), fat oxidation (FO), and (**G** and **H**) carbohydrate oxidation (CO). Thick and jagged lines represent the mean±SEM.

mice. However, even after correction for lean body mass,[28] these differences were not significant. Yet we cannot rule out that these processes are subtly affected in Idol-KO mice and may during a prolonged period contribute to metabolic health.

The indirect calorimetric measurements could suggest elevated energy expenditure fueled by fat oxidation as a preferred energy source in Idol-KO mice. In conjunction with the reduced TG levels in male WTD-fed Idol-KO mice (Figure 1G and 1H), this may point toward increased tissular uptake of lipoprotein-TG–derived fatty acids. To evaluate this possibility, we injected mice with lipoprotein-like particles double-labeled with glycerol tri[^{3}H]oleate and [^{14}C]cholesteryl oleate. We have previously shown that these particles rapidly acquire an array of exchangeable apolipoproteins from serum, including apoE, apoCs, apoAIV, apoAI, apoAII, and apoD, and that the hepatic uptake of their core remnants is mediated by apoE.[18,24] Plasma clearance of both tracers was significantly accelerated in Idol-KO mice (Figure 5A and 5B). The enhanced clearance was mirrored by tissular accumulation of both tracers, with predominant uptake in the liver and adipose tissue (Figure 5C and 5D). No changes in expression of the lipoprotein lipase inhibitor *Angptl4* in WAT or BAT were found in the 21-week WTD-fed mice (Figure VII in the online-only Data Supplement). On the other hand, *Lpl* expression was significantly higher in BAT but not WAT of Idol-KO mice (Figure VII in the online-only Data Supplement). Notably, when corrected for total organ weights, which were lower in the Idol-KO mice (Figure 1C), TG and cholesterol uptake by liver and WAT no longer differed between groups (Figure VIII in the online-only Data Supplement). In contrast,

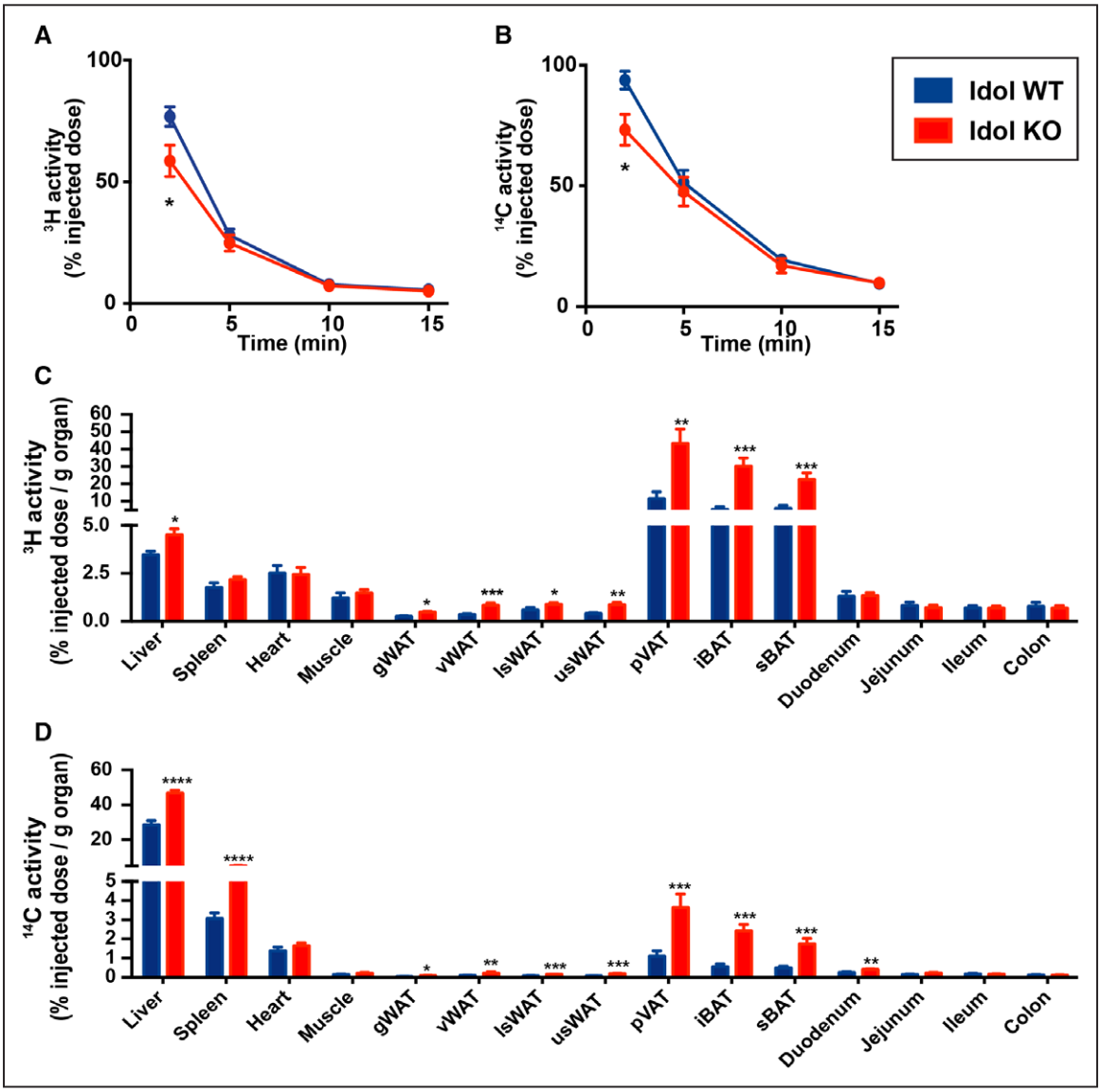

Figure 5. Increased clearance of triglycerides and cholesterol in Idol-KO (knockout) mice. WT (wild type; n=8) and Idol-KO (n=11) male mice were fed a Western-type diet for 5 wk. Mice were fasted for 4 h and injected with reconstituted lipoproteins that contain glycerol tri[^{3}H]oleate and [^{14}C]cholesteryl oleate. At the indicated time points, plasma was collected and radioactivity associated with (**A**) triglycerides and (**B**) cholesterol determined. Subsequently, (**C** and **D**) mice were euthanized and radioactivity in the indicated tissues determined. Each bar or point represents the mean±SEM. gWAT indicates gonadal white adipose tissue; iBAT, interscapular brown adipose tissue; lsWAT, lower subcutaneous white adipose tissue; sBAT, subscapular brown adipose tissue; usWAT, upper subcutaneous white adipose tissue; and vWAT, visceral white adipose tissue. *P<0.01, **P<0.001, ***P<0.0001.

BAT accumulation of both tracers remained significantly increased in Idol-KO mice after correction for organ weight. Elevated uptake of lipids by BAT is in line with increased fat oxidation fueling energy expenditure in Idol-KO mice.

To assess whether the metabolic effects of Idol extend beyond those observed in the inbred Idol-KO mice, we evaluated the metabolic phenotype that is associated with genetically determined variation in Idol expression. To do so, we evaluated the correlation of hepatic Idol expression with metabolic parameters in the BXD inbred mouse strain panel fed a high-fat diet.[19] These inbred strains are derived from an intercross of the C57Bl/6 and DBA mouse strains and allow interrogation of genotype-phenotype associations. Consistent with our current study in global Idol-KO mice, we found that the hepatic expression of Idol positively correlates with body weight (Figure 6A), glucose levels (Figure 6B), WAT content (Figure 6C), and interestingly, negatively correlates with locomotor activity (Figure 6D) in BXDs. In aggregate, our experiments support the involvement of Idol in multiple metabolic syndrome-associated comorbidities and suggest that inhibiting its activity may be beneficial in this setting.

Discussion

The E3 ubiquitin ligase Idol is an established post-transcriptional regulator of the LDLR.[11,12,29] Although the mechanism underlying regulation of this receptor by Idol has been extensively studied, the consequence this has on whole-body metabolism has not been investigated. Therefore, we studied the metabolic role of Idol both during physiological aging and in response to a WTD. Importantly, we discovered that loss of Idol protects mice from multiple comorbidities associated with the metabolic syndrome, including hyperglycemia, obesity, and dyslipidemia. Beneficial metabolic effects of loss of Idol were observed in independent experiments conducted in 2 different animal facilities, in mice of both genders, and both in physiological aging and in response to a WTD. Moreover, our findings in the Idol-KO mice are supported by an association between hepatic *Idol* expression and several metabolic parameters in the BXD mouse genetic reference population.

A simple mechanistic explanation for the beneficial metabolic outcome as a result of loss of Idol would have been decreased dietary fat uptake in the intestine. However, this contention is not supported by our study. It is noteworthy that

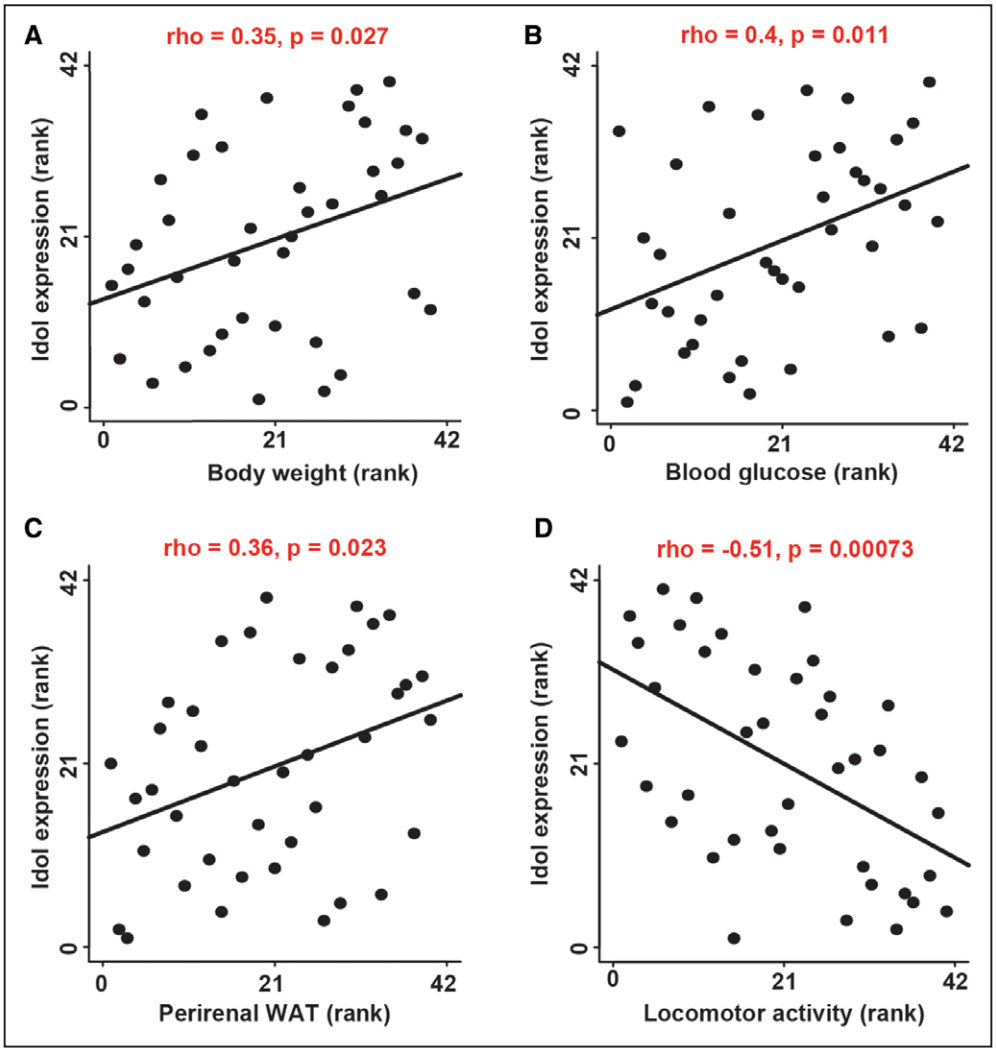

Figure 6. Expression of hepatic Idol correlates with metabolic traits in the BXD mouse strain panel. Spearmann rank-order correlation of hepatic Idol expression with (**A**) body weight, (**B**) plasma glucose level, (**C**) perirenal white adipose tissue (WAT), and (**D**) locomotor activity in male mice (n=5 per strain) fed a high-fat diet of the parental strains C57BL/6 and DBA/2 and of 40 of their intermediate strains.

mice lacking Pcsk9—a secreted factor that like Idol targets the LDLR—do have an altered postprandial response.[30,31] Instead, we propose that the beneficial metabolic control in Idol-KO mice might be, at least in part, attributed to 2 factors: a marked increase in locomotion and potentially a prolonged small increase in energy expenditure and usage of fat as an energy source. Sustained BAT activity may contribute to this, yet we concede that there is no large difference in energy expenditure between control and Idol-KO mice and that the contribution of other mechanisms or involvement of additional tissues (eg, muscle) cannot be excluded. In this regard, it is interesting to point out that one of the most striking differences between WT and Idol-KO mice was locomotor activity, which may suggest involvement of central nervous system Idol activity. Although *Idol* expression is ubiquitous,[11] it is highly expressed in neurons, controls its targets in these cells, and can influence cognitive function in mice.[13,15,32] Although we cannot evaluate the impact of the idol neuronal effects in our experimental setting, our analysis of the BXD cohorts shows that hepatic *Idol* expression correlates with several of the metabolic parameters affected in the global Idol-KO mice. Clearly, development of tissue-specific Idol-KO models will be required to obtain a more precise view of the role of Idol in metabolism.

The most prominent IDOL target is the LDLR—a receptor that controls circulating lipoprotein levels.[11] Recently, the potential involvement of the LDLR in modulating glucose and energy homeostasis has also attracted attention. Namely, several lines of research suggest that increased LDLR levels are associated with a higher incidence of DM2, as seen, for example, in statin-treated individuals and in mice lacking Pcsk9.[3–5,7–10] Conversely, individuals with loss-of-function mutations in the *LDLR* or *ApoB* display favorable glucose handling and reduced incidence of DM2.[2] As such, our current findings with Idol diverge from this dichotomy. We, and others, have demonstrated that in the absence of Idol, the level of the LDLR increases,[11,15,33] but as we show here this is associated with reduced circulating levels of glucose and insulin and overall improved metabolic control. Particularly, in comparison with PCSK9, this was unexpected, as the substrate specificity of IDOL and PCK9 largely overlaps.[12] This discrepancy may be related to tissue-specific effects of these 2 factors. For example, secreted PCSK9 is known to potently regulate hepatic LDLR but less so in the adrenal gland.[34,35] Conversely, in mice, Idol predominantly regulates peripheral but less so hepatic LDLR.[11,16] Increased accumulation of cholesterol in insulin-secreting β-cells, as is the case in the absence of the ABCA1 (ATP-binding cassette subfamily A member 1) efflux transporter in *Abca1*-null mice, results in lipotoxicity and reduced insulin secretion and glycemic control.[36,37] Likewise, poorly controlled uptake of lipoprotein-derived cholesterol via the LDLR pathway, in the absence of Idol or Pcsk9, could be anticipated to lead to a similar outcome. Therefore, the difference between Idol-KO and Pcsk9-KO mice with respect to glycemic control suggests that pancreatic Idol activity is limited and warrants further studies on the role of Pcsk9 in this organ.

An important aspect of our study pertains to the therapeutic potential of targeting IDOL. To date, IDOL inhibition has been considered as a cholesterol-lowering target owing to its ability to increase abundance of the LDLR.[12] This notion is further supported by human genetic studies that demonstrate an association between genetic variation in *IDOL* and circulating cholesterol levels in humans[17,38,39] and antisense *IDOL* RNA studies in nonhuman primates.[16] Moreover, the ability of IDOL to regulate LDLR abundance in the brain affects clearance of the amyloid- β peptide and may, therefore, be beneficial in the setting of Alzheimer disease.[33] Our current study demonstrates that loss of Idol also decreases diet-induced obesity, circulating levels of TC, TG, and glucose in mice, thus expanding the possible benefit that may be attained by Idol inhibition.

In conclusion, we demonstrate an effect of Idol in the development of metabolic syndrome in mice. With the global burden of this pathological condition rising at an alarming rate, our current findings support further studies into the mechanistic involvement and pathophysiological role of IDOL in the metabolic syndrome.

Acknowledgments

We thank the members of the Zelcer group, Esther Lutgens and Irith Koster, for their comments and suggestions. We thank Lianne van der Wee-Pals for her excellent technical assistance, Peter Tontonoz for the *Idol*$^{(-/-)}$ mice, and the animal caretakers of the animal facility of the Academic Medical Center for their assistance.

Sources of Funding

V. Sorrentino is supported by the EPFL Fellows program cofunded by the Marie Skłodowska-Curie, Horizon 2020 grant agreement (665667). S. Kooijman is supported by a Dekker-Junior postdoc grant of the Dutch Heart Foundation (2017T016). P.C.N. Rensen is supported by the Netherlands CardioVascular Research Initiative: the Dutch Heart Foundation, Dutch Federation of University Medical Centers, the Netherlands Organisation for Health Research and Development, and the Royal Netherlands Academy of Sciences (CVON-GENIUS-II). N. Zelcer is an established investigator of the Dutch Heart Foundation (2013T111) and is supported by a European Research Council Consolidator grant (617376) from the European Research Council.

Disclosures

None.

References

1. Brown MS, Goldstein JL. A receptor-mediated pathway for cholesterol homeostasis. *Science*. 1986;232:34–47.
2. Besseling J, Kastelein JJ, Defesche JC, Hutten BA, Hovingh GK. Association between familial hypercholesterolemia and prevalence of type 2 diabetes mellitus. *JAMA*. 2015;313:1029–1036. doi: 10.1001/jama.2015.1206.
3. Ridker PM, Pradhan A, MacFadyen JG, Libby P, Glynn RJ. Cardiovascular benefits and diabetes risks of statin therapy in primary prevention: an analysis from the JUPITER trial. *Lancet*. 2012;380:565–571. doi: 10.1016/S0140-6736(12)61190-8.
4. Sattar N, Preiss D, Murray HM, et al. Statins and risk of incident diabetes: a collaborative meta-analysis of randomised statin trials. *Lancet*. 2010;375:735–742. doi: 10.1016/S0140-6736(09)61965-6.
5. Casula M, Mozzanica F, Scotti L, Tragni E, Pirillo A, Corrao G, Catapano AL. Statin use and risk of new-onset diabetes: a meta-analysis of observational studies. *Nutr Metab Cardiovasc Dis*. 2017;27:396–406. doi: 10.1016/j.numecd.2017.03.001.
6. Seidah NG, Awan Z, Chrétien M, Mbikay M. PCSK9: a key modulator of cardiovascular health. *Circ Res*. 2014;114:1022–1036. doi: 10.1161/CIRCRESAHA.114.301621.
7. Schmidt AF, Swerdlow DI, Holmes MV, et al. *Lancet Diabetes Endocrinol*. 2017;5:97–105. doi:10.1016/S2213-8587(16)30396-5.
8. Ference BA, Robinson JG, Brook RD, Catapano AL, Chapman MJ, Neff DR, Voros S, Giugliano RP, Davey Smith G, Fazio S, Sabatine MS. Variation

in PCSK9 and HMGCR and risk of cardiovascular disease and diabetes. *N Engl J Med*. 2016;375:2144–2153. doi: 10.1056/NEJMoa1604304.
9. Mbikay M, Sirois F, Mayne J, Wang GS, Chen A, Dewpura T, Prat A, Seidah NG, Chretien M, Scott FW. PCSK9-deficient mice exhibit impaired glucose tolerance and pancreatic islet abnormalities. *FEBS Lett*. 2010;584:701–706. doi: 10.1016/j.febslet.2009.12.018.
10. Mbikay M, Sirois F, Gyamera-Acheampong C, Wang GS, Rippstein P, Chen A, Mayne J, Scott FW, Chrétien M. Variable effects of gender and Western diet on lipid and glucose homeostasis in aged PCSK9-deficient C57BL/6 mice CSK9PC57BL/6. *J Diabetes*. 2015;7:74–84. doi: 10.1111/1753-0407.12139.
11. Zelcer N, Hong C, Boyadjian R, Tontonoz P. LXR regulates cholesterol uptake through Idol-dependent ubiquitination of the LDL receptor. *Science*. 2009;325:100–104. doi: 10.1126/science.1168974.
12. Sorrentino V, Zelcer N. Post-transcriptional regulation of lipoprotein receptors by the E3-ubiquitin ligase inducible degrader of the low-density lipoprotein receptor. *Curr Opin Lipidol*. 2012;23:213–219. doi: 10.1097/MOL.0b013e3283532947.
13. Olsson PA, Korhonen L, Mercer EA, Lindholm D. MIR is a novel ERM-like protein that interacts with myosin regulatory light chain and inhibits neurite outgrowth. *J Biol Chem*. 1999;274:36288–36292.
14. Poirier S, Mayer G, Benjannet S, Bergeron E, Marcinkiewicz J, Nassoury N, Mayer H, Nimpf J, Prat A, Seidah NG. The proprotein convertase PCSK9 induces the degradation of low density lipoprotein receptor (LDLR) and its closest family members VLDLR and ApoER2. *J Biol Chem*. 2008;283:2363–2372. doi: 10.1074/jbc.M708098200.
15. Hong C, Duit S, Jalonen P, Out R, Scheer L, Sorrentino V, Boyadjian R, Rodenburg KW, Foley E, Korhonen L, Lindholm D, Nimpf J, van Berkel TJ, Tontonoz P, Zelcer N. The E3 ubiquitin ligase IDOL induces the degradation of the low density lipoprotein receptor family members VLDLR and ApoER2. *J Biol Chem*. 2010;285:19720–19726. doi: 10.1074/jbc.M110.123729.
16. Hong C, Marshall SM, McDaniel AL, et al. The LXR-Idol axis differentially regulates plasma LDL levels in primates and mice. *Cell Metab*. 2014;20:910–918. doi: 10.1016/j.cmet.2014.10.001.
17. Sorrentino V, Fouchier SW, Motazacker MM, Nelson JK, Defesche JC, Dallinga-Thie GM, Kastelein JJ, Kees Hovingh G, Zelcer N. Identification of a loss-of-function inducible degrader of the low-density lipoprotein receptor variant in individuals with low circulating low-density lipoprotein. *Eur Heart J*. 2013;34:1292–1297. doi: 10.1093/eurheartj/ehs472.
18. Rensen PC, van Dijk MC, Havenaar EC, Bijsterbosch MK, Kruijt JK, van Berkel TJ. Selective liver targeting of antivirals by recombinant chylomicrons–a new therapeutic approach to hepatitis B. *Nat Med*. 1995;1:221–225.
19. Andreux PA, Williams EG, Koutnikova H, Houtkooper RH, Champy MF, Henry H, Schoonjans K, Williams RW, Auwerx J. Systems genetics of metabolism: the use of the BXD murine reference panel for multiscalar integration of traits. *Cell*. 2012;150:1287–1299. doi: 10.1016/j.cell.2012.08.012.
20. Wu Y, Williams EG, Dubuis S, Mottis A, Jovaisaite V, Houten SM, Argmann CA, Faridi P, Wolski W, Kutalik Z, Zamboni N, Auwerx J, Aebersold R. Multilayered genetic and omics dissection of mitochondrial activity in a mouse reference population. *Cell*. 2014;158:1415–1430. doi: 10.1016/j.cell.2014.07.039.
21. Levels JHM, Lemaire LCJM, van den Ende AE, van Deventer SJH, van Lanschot JJB. Lipid composition and lipopolysaccharide binding capacity of lipoproteins in plasma and lymph of patients with systemic inflammatory response syndrome and multiple organ failure. *Crit Care Med*. 2003;31:1647–1653. doi:10.1097/01.CCM.0000063260.07222.76.
22. Galarraga M, Campión J, Muñoz-Barrutia A, Boqué N, Moreno H, Martínez JA, Milagro F, Ortiz-de-Solórzano C. Adiposoft: automated software for the analysis of white adipose tissue cellularity in histological sections. *J Lipid Res*. 2012;53:2791–2796. doi: 10.1194/jlr.D023788.
23. Kooijman S, Wang Y, Parlevliet ET, Boon MR, Edelschaap D, Snaterse G, Pijl H, Romijn JA, Rensen PC. Central GLP-1 receptor signalling accelerates plasma clearance of triacylglycerol and glucose by activating brown adipose tissue in mice. *Diabetologia*. 2015;58:2637–2646. doi: 10.1007/s00125-015-3727-0.
24. Berbée JF, Boon MR, Khedoe PP, et al. Brown fat activation reduces hypercholesterolaemia and protects from atherosclerosis development. *Nat Commun*. 2015;6:6356. doi: 10.1038/ncomms7356.
25. Peet DJ, Turley SD, Ma W, Janowski BA, Lobaccaro JM, Hammer RE, Mangelsdorf DJ. Cholesterol and bile acid metabolism are impaired in mice lacking the nuclear oxysterol receptor LXR alpha. *Cell*. 1998;93:693–704.
26. Cohen P, Spiegelman BM. Brown and beige fat: molecular parts of a thermogenic machine. *Diabetes*. 2015;64:2346–2351. doi: 10.2337/db15-0318.
27. Enerbäck S, Jacobsson A, Simpson EM, Guerra C, Yamashita H, Harper ME, Kozak LP. Mice lacking mitochondrial uncoupling protein are cold-sensitive but not obese. *Nature*. 1997;387:90–94. doi: 10.1038/387090a0.
28. van Beek L, van Klinken JB, Pronk AC, van Dam AD, Dirven E, Rensen PC, Koning F, Willems van Dijk K, van Harmelen V. The limited storage capacity of gonadal adipose tissue directs the development of metabolic disorders in male C57Bl/6J mice. *Diabetologia*. 2015;58:1601–1609. doi: 10.1007/s00125-015-3594-8.
29. Sorrentino V, Nelson JK, Maspero E, Marques AR, Scheer L, Polo S, Zelcer N. The LXR-IDOL axis defines a clathrin-, caveolae-, and dynamin-independent endocytic route for LDLR internalization and lysosomal degradation. *J Lipid Res*. 2013;54:2174–2184. doi: 10.1194/jlr.M037713.
30. Le May C, Kourimate S, Langhi C, Chétiveaux M, Jarry A, Comera C, Collet X, Kuipers F, Krempf M, Cariou B, Costet P. Proprotein convertase subtilisin kexin type 9 null mice are protected from postprandial triglyceridemia. *Arterioscler Thromb Vasc Biol*. 2009;29:684–690. doi: 10.1161/ATVBAHA.108.181586.
31. Roubtsova A, Munkonda MN, Awan Z, Marcinkiewicz J, Chamberland A, Lazure C, Cianflone K, Seidah NG, Prat A. Circulating proprotein convertase subtilisin/kexin 9 (PCSK9) regulates VLDLR protein and triglyceride accumulation in visceral adipose tissue. *Arterioscler Thromb Vasc Biol*. 2011;31:785–791. doi: 10.1161/ATVBAHA.110.220988.
32. Gao J, Marosi M, Choi J, Achiro JM, Kim S, Li S, Otis K, Martin KC, Portera-Cailliau C, Tontonoz P. The E3 ubiquitin ligase IDOL regulates synaptic ApoER2 levels and is important for plasticity and learning. *Elife*. 2017;6:1741. doi:10.7554/eLife.29178.
33. Choi J, Gao J, Kim J, Hong C, Kim J, Tontonoz P. The E3 ubiquitin ligase Idol controls brain LDL receptor expression, ApoE clearance, and Aβ amyloidosis. *Sci Transl Med*. 2015;7:314ra184. doi: 10.1126/scitranslmed.aad1904.
34. Lagace TA, Curtis DE, Garuti R, McNutt MC, Park SW, Prather HB, Anderson NN, Ho YK, Hammer RE, Horton JD. Secreted PCSK9 decreases the number of LDL receptors in hepatocytes and in livers of parabiotic mice. *J Clin Invest*. 2006;116:2995–3005. doi: 10.1172/JCI29383.
35. Grefhorst A, McNutt MC, Lagace TA, Horton JD. Plasma PCSK9 preferentially reduces liver LDL receptors in mice. *J Lipid Res*. 2008;49:1303–1311. doi: 10.1194/jlr.M800027-JLR200.
36. Brunham LR, Kruit JK, Verchere CB, Hayden MR. Cholesterol in islet dysfunction and type 2 diabetes. *J Clin Invest*. 2008;118:403–408. doi: 10.1172/JCI33296.
37. Kruit JK, Wijesekara N, Fox JE, et al. Islet cholesterol accumulation due to loss of ABCA1 leads to impaired exocytosis of insulin granules. *Diabetes*. 2011;60:3186–3196. doi: 10.2337/db11-0081.
38. Teslovich TM, Musunuru K, Smith AV, et al. Biological, clinical and population relevance of 95 loci for blood lipids. *Nature*. 2010;466:707–713. doi: 10.1038/nature09270.
39. Weissglas-Volkov D, Calkin AC, Tusie-Luna T, Sinsheimer JS, Zelcer N, Riba L, Tino AM, Ordoñez-Sánchez ML, Cruz-Bautista I, Aguilar-Salinas CA, Tontonoz P, Pajukanta P. The N342S MYLIP polymorphism is associated with high total cholesterol and increased LDL receptor degradation in humans. *J Clin Invest*. 2011;121:3062–3071. doi: 10.1172/JCI45504.

Highlights

- Idol loss protects mice from diet-induced obesity, hyperglycemia, and dyslipidemia.
- Idol absence limits diet-induced hepatic and brown adipose tissue fat accumulation.
- Brown adipose tissue fatty acid uptake is increased in Idol knockout mice.
- Liver *Idol* expression correlates with metabolic parameters in the BXD mouse panel.